JOURNAL OF CATALYSIS **180,** 184–193 (1998)
ARTICLE NO. CA982288

Density Functional Theory (DFT) Studies of C_1 and C_2 Hydrocarbons Species on Pt Clusters

R. M. Watwe, B. E. Spiewak,[1] R. D. Cortright, and J. A. Dumesic[2]

Department of Chemical Engineering, University of Wisconsin, Madison, Wisconsin 53706

Received March 25, 1998; revised September 23, 1998; accepted September 30, 1998

Quantum chemical calculations were performed using density functional theory to study interactions of C_1 and C_2 hydrocarbons with 10-atom Pt clusters. The heats of ethylene adsorption to form di-σ- and π-adsorbed species were calculated to be -171 kJ/mol and -103 kJ/mol, respectively, at 298 K. The calculated heat is -109 kJ/mol for the formation of ethylidyne species from ethylene adsorption, with the formation of gas phase dihydrogen at 298 K. The heat of adsorption of acetylene to form molecular, di-σ/π-adsorbed species is -209 kJ/mol, and the heat of formation of di-σ/π vinylidene species is -278 kJ/mol at 298 K. The calculated structural parameters of these species agree with the available experimental data. The same 10-atom platinum cluster is used to calculate the heats of adsorption of various other hydrocarbon species which may be reactive intermediates for hydrocarbon conversion reactions. These species include vinyl, methyl, ethyl, methylene, ethylidene, and ethylylidene species.

Key Words: **microcalorimetry; ethylene; acetylene; adsorption; platinum; DFT.**

INTRODUCTION

Rationale

Reactions of hydrocarbons on metal catalysts (e.g., Pt) are of importance in the chemical and petrochemical industries (e.g., (1, 2)). Accordingly, significant experimental efforts have been made in the catalysis and surface science communities to study the interactions of small hydrocarbons with various metal surfaces (e.g., (3, 4)). In addition, theoretical methods involving electronic structure calculations have recently become viable tools for investigating the chemistry of catalytic systems (e.g., (5–8)). The application of these theoretical techniques requires calibration of the method (level of theory, basis set, cluster size, and shape) through the prediction of chemistry that has been observed experimentally, such as heats of adsorption. The results of these calibrated theoretical methods, combined with experimental results, provide further insight into factors controlling catalyst performance.

In the present paper, we address possible reaction intermediates involved in ethane hydrogenolysis over platinum. This reaction has been studied by various authors (e.g., (9–12)), and the literature related to this reaction forms a foundation for studies involving microcalorimetric, kinetic, and quantum chemical studies of C_2 species on platinum. We begin our studies with the adsorption of ethylene and acetylene on platinum. We will show that the experimentally measured heats of interaction of these molecules with platinum at various temperatures can be explained using quantum chemical calculations, employing density functional theory (DFT) for Pt_{10} clusters. These Pt_{10} clusters are then used to estimate the energetics of various hydrocarbon fragments postulated to be intermediates in the hydrogenolysis of ethane over platinum. Importantly, these intermediates are difficult to examine by common experimental techniques, and one has to rely on theoretical calculations to predict the structures and energetics of these species. In a related paper, the heats of adsorption predicted from quantum chemical studies are combined with kinetic measurements to develop a quantitative kinetic description of ethane hydrogenolysis over supported Pt catalysts (13).

Carter and Koel (14) published a table of energetics for gas-phase C_1 and C_2 hydrocarbon species and the interaction of these species with Pt(111). Similar to this present paper, these investigators presented energetics of species which could be determined experimentally (e.g., from TPD results and data compiled by Benson (15)), and they presented an approximation scheme to estimate the energetics of the species that have not been observed experimentally.

Literature

The interactions of ethylene with single crystal platinum surfaces and supported platinum catalysts have been widely studied, and the results of these investigations show distinct surface species depending on temperature. For example, ultrahigh vacuum studies of ethylene adsorption on Pt(111) have identified π-bonded ethylene species at temperatures

[1] Present address: 3M Corporation, St. Paul, MN 55144.
[2] To whom correspondence should be addressed.

0021-9517/98 $25.00

below 52 K (16), di-σ-bonded ethylene species from 100–250 K (17–20), and ethylidyne species from 280–450 K (17, 21, 22). Importantly, Sheppard and De La Cruz have shown (23) that results comparable to those obtained on single crystal metal surface are found when ethylene is dosed onto supported platinum catalysts. For example, infrared spectra show the presence of π-bonded and di-σ-bonded species when ethylene is dosed onto silica- and alumina-supported platinum at low temperatures (<195 K), whereas ethylidyne species form at room temperature (23).

Similar to ethylene adsorption on platinum at low temperatures (<250 K), acetylene has been shown to adsorb associatively with its C–C axis parallel to the platinum surface (24). On a Pt(111) surface, acetylene is thought to form two σ-bonds and one π-bond to three platinum atoms (19, 24–26) in threefold hollow sites (26, 27). Acetylene has been shown to adsorb associatively at higher temperatures (>280 K) with its C–C axis normal to the platinum surface (18, 19, 21, 22, 24, 28, 29). Vinylidene species have been suggested to be responsible for this type of adsorption (18, 20, 21, 29–31); however, ethylidyne species (22, 28), which form in the presence of surface hydrogen (18, 19, 22, 24, 25, 29, 32–34), and di-σ/π-vinylidene species (19, 32) have also been proposed to form.

The strengths with which the aforementioned species interact with platinum have been probed with microcalorimetry. For example, Dumesic and co-workers (35–38) have used heat-flux microcalorimetry to measure the heat of ethylene and acetylene adsorption on supported platinum catalysts and platinum powder, and King and co-workers (39–41) have used ultrahigh vacuum microcalorimetry to measure the heat of ethylene adsorption on platinum single crystals. These studies were performed on platinum surfaces at temperatures near 300 K, where ethylene adsorbs dissociatively to form ethylidyne species and surface hydrogen.

METHODS

In the present investigation, the interactions of C_1 and C_2 species with a platinum cluster containing 10 atoms were studied using DFT methods. Such DFT methods have proven to be useful to predict accurate geometries and reasonable energetics for molecules containing transition metals (5, 42–45). The currently available DFT methods use few semi-empirical parameters in conjunction with more advanced functionals to give an adequate description of nonlocal effects in electron exchange and correlation interactions.

The DFT calculations were carried out using DEC workstations, with PS-GVB software (Schrodinger, Inc.) (46). This software uses a pseudo-spectral method to evaluate the various integrals. It combines both a basis set and a physical space grid, thus retaining the speed of discrete methods and the smoothing properties of continuous functions. The chosen DFT method uses a hybrid method employing Becke's three-parameters approach, B3LYP (47). This functional combines the exact HF exchange, Slater's local exchange functional, Becke's 1988 nonlocal gradient correction to the exchange functional, with the correlation functionals of Vosko–Wilk–Nusair (VWN) and Lee–Yang–Parr (LYP).

The basis set employed in all calculations (LACVP**) uses an effective core potential on all Pt atoms, developed at Los Alamos National Laboratory by Hay and Wadt (48). The electrons treated explicitly on Pt are the outermost core and valence electrons ($5s^2\ 5p^6\ 5d^9\ 6s^1$), with the remaining core electrons treated with effective core potentials which account for mass-velocity and relativistic effects. The inclusion of outermost core electrons with the valence electrons is necessary because these core orbitals have similar sizes as the valence orbitals. Use of pseudo-potentials to replace the outermost core electrons leads to quantitatively different results, as will be shown later in this paper. The C and H atoms have been treated with the 6-31G** basis set (49), with all electrons being treated explicitly.

Electronic energies were calculated for all clusters by conducting full geometry optimizations. The Pt-Pt bond distances in these geometry optimizations were not constrained, since relaxation and adsorption-induced reconstruction effects are common for small particles (50–52). The electronic energies calculated after geometry optimizations were corrected for basis set superposition error (BSSE) using Boys–Bernardi counterpoise calculations for all adsorbate/cluster models (53). This correction is ~10–12 kJ/mol per bond between the adsorbate and the cluster.

The change in electronic energy for adsorption ($\Delta E_{\text{electronic}}$) is defined as

$$\Delta E_{\text{electronic}} = E_{\text{cluster/adsorbate}} - (E_{\text{cluster}} + E_{\text{adsorbate}}),$$

where $E_{\text{cluster/adsorbate}}$ is the electronic energy of the adsorbate on the cluster, E_{cluster} is the electronic energy of the bare cluster (Pt_{10}), and $E_{\text{adsorbate}}$ is the electronic energy of the gas-phase adsorbate (C_2H_4, C_2H_2, etc.).

Calculated heats of adsorption at higher temperature facilitate comparison with the experimentally measured values and also can be used for estimation of kinetic parameters for ethane hydrogenolysis on platinum catalysts. Accordingly, frequency calculations were performed to compute zero-point vibration and enthalpy corrections and the heats of adsorption were estimated at 298 K and 623 K. As an approximation, we assume that the vibrational frequencies of the surface adsorbate are the same as those of the corresponding gas phase radical to calculate the enthalpy and zero-point energy corrections. The heat of adsorption ($\Delta H_{\text{ads}}(T)$) to form a particular surface species at temperature T is thus estimated by

$$\Delta H_{\text{ads}}(T) = \Delta E_{\text{electronic}} + \Delta ZPE + \Delta H(T)_{\text{enthalpy corrections}},$$

where ΔZPE and $\Delta H(T)_{\text{enthalpy corrections}}$ are the changes in zero-point energies and enthalpy corrections for the corresponding gas-phase reaction of radical species. In this correction we assume that the thermal energy loss from reduction of translational and rotational modes upon adsorption is compensated by the thermal energy acquisition from increased vibrational modes attributed to frustrated translation and rotation of the adsorbate on the cluster.

RESULTS/DISCUSSION

Density Functional Theory Calculations

Dissociation energy of $PtCH_2^+$. Information about the accuracy of the present theoretical calculations may be inferred by investigating the dissociation energy of the $PtCH_2^+$ complex cation. The reported experimental value for the dissociation of this cation is 479.5 kJ/mol ± 4.2 kJ/mol (54). The value for this dissociation energy is calculated to be 504.2 kJ/mol, using the B3LYP functional, the LACVP** basis set, and correcting for changes in zero-point energies. This comparision shows that the DFT method predicts overbinding between the transition metal and the adsorbate, but this difference is in general agreement with the accuracy limit of 20 kJ/mol suggested by van Santen and Neurock (5) for DFT cluster calculations.

Pt_{10} cluster. The Pt_{10} cluster used in this study has 10 atoms arranged into three layers resembling (111) planes, as shown in Fig. 1. This cluster has threefold, twofold, and atop adsorption sites. The Pt-Pt distances in the optimized cluster range from 2.56 to 2.88 Å, with an average value of 2.72 Å. The distance in bulk Pt metal is 2.77 Å. The atoms in the center of the four faces are slightly puckered out from the center of the cluster. This cluster has been described in detail elsewhere (55).

Boyanov and Morrison have studied the structures of platinum clusters containing 10–25 atoms on Y zeolite, using X-ray absorption (XANES and EXAFS) and X-ray photoelectron spectroscopy (56). They report the average interatomic distance to be 2.70 Å, and they conclude that this bond contraction of 0.07 Å compared to bulk Pt is intrinsic to the cluster with no effect from zeolite support.

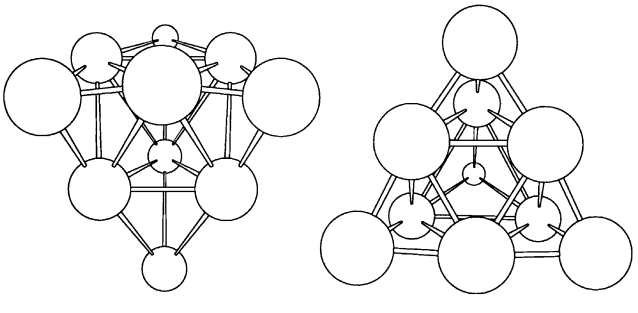

FIG. 1. Two views of a 10-atom platinum cluster.

TABLE 1

Predicted Zero-Point Energies and Enthalpies Corrections for Gas-Phase Species and Adsorbate Fragments

Gas-phase species or fragments	Multiplicity	Zero-point energy (kJ/mol)	Enthalpy correction to 298 K (kJ/mol)	Enthalpy correction to 623 K (kJ/mol)
C_2H_4	1	134	10	29
C_2H_6	1	197	11	34
CH_4	1	118	10	24
H_2	1	27	9	18
CH	4	19	9	18
CH_2	3	46	10	22
CH_3	2	78	11	25
C_2H_5	2	158	12	35
C_2H_4	3	104	18	42
$CHCH_3$	4	124	12	32
$CHCH_2$	4	91	11	30
CCH_3	4	98	10	27
C_2H_2	5	52	13	30
C_2H_2	1	70	10	27
CCH_2	3	65	10	25

Koningsberger and co-workers report from EXAFS measurements that the interatomic distance is 2.74 Å for a cluster of 4–5 Pt atoms with coordination number of 3.7 in L-zeolite (57). Sachtler and co-workers have reported a value of 2.64 Å for platinum particles with average coordination number of 7.7 (58). The results from these experimental studies are in agreement with the predictions from the present study that the average Pt-Pt distance of 2.72 Å in Pt_{10} clusters is shorter than the value of 2.77 Å in bulk Pt metal.

Gas-phase species. Table 1 shows the zero-point energies and enthalpy corrections for the gas-phase compounds and the gas-phase radicals corresponding to the adsorbates of this present investigation. This table also lists the spin multiplicities for the different gas-phase species.

Optimization of the geometry of gaseous ethylene gives C-C and C-H bond lengths of 1.33 and 1.09 Å, respectively, and the H-C-H angle is 116°. These values are in agreement with the experimental values of 1.34 Å, 1.09 Å, and 117.8°, respectively. The calculated C-C and C-H bond lengths for gaseous acetylene are 1.20 and 1.07 Å, and the H-C-C angle is 180°. The corresponding experimental values are 1.20 Å, 1.06 Å, and 180°.

Ethylene-Pt_{10}. Various theoretical studies have addressed the chemisorption of ethylene on platinum (8, 21, 59, 60). The optimized geometry for di-σ-ethylene (μ_2, η^2-ethene) is shown in Fig. 2. The calculated C-C bond length for this species is 1.50 Å, in agreement with experimental values (1.48–1.52 Å) (61, 62). The calculated value of the C-C bond length is close to the C-C bond length in ethane (1.54 Å) and considerably longer than that in ethylene (1.34 Å), indicating rehybridization of the C-C bond

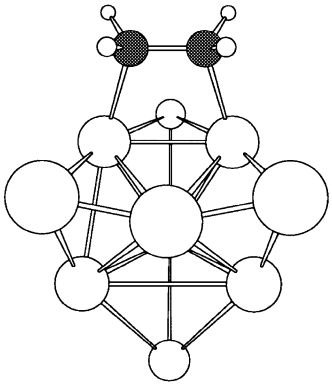

FIG. 2. Structural model for di-σ-adsorbed ethylene on a Pt_{10} cluster.

from sp^2 to sp^3. This rehybridization has been seen experimentally on Pt(111) at low temperatures (23, 24). The calculated heat of ethylene adsorption to form this di-σ-adsorbed species is -171 kJ/mol at 298 K. Results from recent LEED studies of ethylene adsorbed on Pt(111) suggest that the C-C axis is tilted with respect to the surface plane by about 22° (63). We do not observe this geometry for the di-σ-adsorbed species.

Ethylene adsorption on atop sites can also lead to π-adsorbed species (η^2-ethene), and Fig. 3 shows two types of π-adsorption that were found on the Pt_{10} cluster. The first π-adsorbed species has the C-C axis of ethylene oriented parallel to the edge of the platinum cluster (Fig. 3a), while the second species has the C-C axis oriented perpendicular to the edge (Fig. 3b). The C-C bond length is 1.41 Å for both structures, in agreement with NEXAFS results which give a value of 1.41 Å (64).

The calculated heat of ethylene adsorption at 298 K to form the first type of π-adsorbed species is -103 kJ/mol, and the heat for the second species is -137 kJ/mol. It has been shown experimentally that ethylene forms π-adsorbed species on the (110) and (210) surfaces of Pt, for which the surface atoms have coordination numbers of 7 and 6, respectively (65, 66). A theoretical study by Paul and Sautet showed that the π-adsorbed species is more stable than the di-σ-adsorbed species for coordination numbers lower than or equal to 7 (67). In the present study the coordination number of the Pt atoms on which ethylene is adsorbed is 6.

For more densely packed surfaces, such as Pt(111), it has been shown that the di-σ-adsorbed species is more stable than the π-adsorbed species. Ethylene adsorbs as π-bonded species at low temperature and rehybridizes at temperatures above 52 K into di-σ species on Pt(111) (16, 21, 28). The first type of π-adsorbed species (with the C-C axis oriented parallel to the edge of the cluster) may be a better representation of π-adsorbed species on such a densely packed surface, and the heat associated with this first type of π-adsorbed species is considerably lower than the value for the di-σ-adsorbed species. In another theoretical study using semi-empirical theory, the di-σ-adsorbed species was found to be more stable than π-adsorbed species on Pt(111) by 50 kJ/mol, which agrees with the difference in the present study of 46 kJ/mol (68).

Table 2 compares the heats of adsorption of ethylene calculated in the present study to the experimentally measured heats of adsorption on platinum (35, 39). Microcalorimetric results for ethylene adsorption on platinum powders at 173 K show a heat of -120 kJ/mol (35). Studies of ethylene adsorption on Pt at temperatures between 100 and 270 K have shown that ethylene adsorbs associatively as a combination of di-σ-adsorbed and π-adsorbed species (23, 24). Recently, similar initial heats of adsorption were observed for ethylene adsorption on silica-supported platinum at temperatures lower than 200 K (69). Low temperature infrared spectroscopic investigations of this same Pt/SiO_2 catalyst showed that these observed heats may, in fact, be attributed to the formation of di-σ- and π-adsorbed ethylene species (69). Importantly, the observed heat of

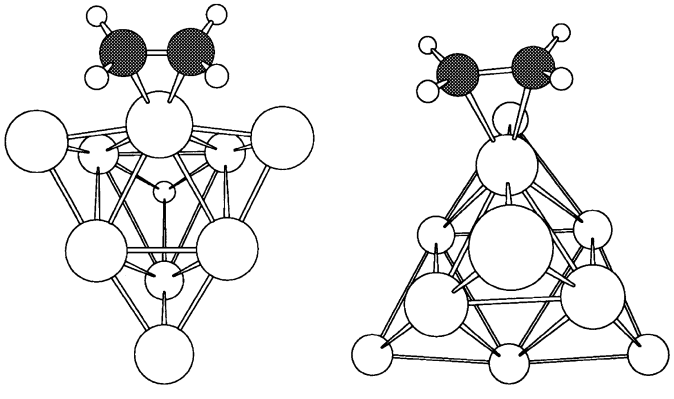

FIG. 3. Structural models for two modes of π-adsorbed ethylene on Pt_{10} clusters.

TABLE 2

Comparison of Experimental and Theoretical Results

Reaction	Enthalpy change (kJ/mol) This work 298 K	King and co-workers (39)	Dumesic and co-workers (35)
$Pt_{10} + C_2H_4 = Pt_{10}$-$C_2H_4$ (di-σ-ethylene, Fig. 2)	-171	-136	-120
$Pt_{10} + C_2H_4 = Pt_{10}$-$C_2H_4$ (π-ethylene, Fig. 3(a))	-103	-120	di-$\sigma + \pi$ species
$Pt_{10} + C_2H_4 = Pt_{10}$-$CCH_3 + 0.5\ H_2$ (ethylidyne, Fig. 4(a))	-127	-125	-115
$Pt_{10} + C_2H_2 = Pt_{10}$-$C_2H_2$ (di-σ/π-acetylene, Fig. 5(a))	-209		-210
$Pt_{10} + C_2H_2 = Pt_{10}$-$CCH_2$ (di-σ/π-vinylidene, Fig. 5(b))	-278	-290	

−120 kJ/mol suggests that adsorption of ethylene on platinum at 173 K is a nonequilibrated process. Accordingly, the observed heat of −120 kJ/mol reported by Spiewak *et al.* can be attributed to the average heat for the formation of a combination of di-σ- and π-adsorbed species (35). King and coworkers have reported a heat of ethylene adsorption equal to −136 kJ/mol to form di-σ-adsorbed species and a value of −120 kJ/mol to form π-adsorbed species on a Pt(110)(2 × 1) surface at room temperature (39).

Ethylidyne-Pt_{10}. Studies of the interactions of ethylene with Pt(111) at temperatures above 280 K indicate that ethylene adsorbs dissociatively and rearranges such that its C-C axis is oriented normal to the surface (23). The resulting ethylidyne species forms bonds with three surface atoms. The ethylidyne (μ_3-ethylidyne) species prefers the threefold FCC hollow site on platinum. Our calculations for the adsorbed ethylidyne species, shown in Fig. 4, give a C-C bond length of 1.52 Å and C-Pt bond lengths of 1.98 Å. The hydrogen atoms point towards the bridge positions on the Pt cluster (Fig. 4a). This geometry agrees with results from LEED reported by Somorjai and co-workers (22), which indicate a C-C length of 1.50 ± 0.05 Å and Pt-C lengths of 2.00 ± 0.05 Å.

The heat of adsorption of ethylene to form ethylidyne species and gas phase dihydrogen is calculated to be −127 kJ/mol at 298 K. Another configuration of ethylidyne species with hydrogen atoms pointing towards the atop positions of the platinum cluster (Fig. 4b) gives a heat of adsorption of −117 kJ/mol (see Table 3). The small energy difference (10 kJ/mol) between the two structures suggests that rotation of the methyl group about C-C axis may be facile. This prediction agrees with the absence of hydrogen-related features in LEED data at 90 K (70).

Table 2 compares theoretical and experimental heats to form ethylidyne and gas-phase dihydrogen from the adsorption of ethylene on platinum at room temperature. Studies of ethylene adsorption on Pt near room temperature have shown that ethylene adsorbs dissociatively to form ethylidyne species and atomic adsorbed hydrogen (23, 24). King and coworkers reported a heat of −170 kJ/mol for adsorption of ethylene on Pt(110)(2 × 1) (39) while the microcalorimetric results for ethylene interaction with platinum powder at 303 K give a heat of −160 kJ/mol (35). Since the heat of adsorption of H_2 on Pt may be taken to be −90 kJ/mol (37, 71), the observed heats reported by King and coworkers and Spiewak *et al.*, correspond to values of −125 kJ/mol and −115 kJ/mol, respectively, for the formation of ethylidyne species on Pt and gaseous dihydrogen. These experimental values are in good agreement with the DFT result that predicts the heat of formation of ethylidyne species and gas phase dihydrogen to be −127 kJ/mol at 298 K (see Table 2).

The lower heat observed by Spiewak *et al.* (35) may be the result of nonequilibrated adsorption of ethylene on Pt powder at 303 K, and this reported heat corresponds to an

TABLE 3

DFT Results for Adsorption of C_1 and C_2 Hydrocarbons Species on Pt_{10} Clusters

Reaction	$\Delta E_{electronic}$ (kJ/mol)	ΔH (298 K) (kJ/mol)	ΔH (623 K) (kJ/mol)
$Pt_{10} + C_2H_4 = Pt_{10}\text{-}C_2H_4$ (di-σ ethylene, Fig. 2)	−149	−171	−166
$Pt_{10} + C_2H_4 = Pt_{10}\text{-}C_2H_4$ (π ethylene, Fig. 3(a))	−103	−103	−103
$Pt_{10} + C_2H_4 = Pt_{10}\text{-}C_2H_4$ (π ethylene, Fig. 3(b))	−137	−137	−137
$Pt_{10} + C_2H_4 = Pt_{10}\text{-}CCH_3 + 0.5\ H_2$ (ethylidyne, Fig. 4(a))	−109	−127	−124
$Pt_{10} + C_2H_4 = Pt_{10}\text{-}CCH_3 + 0.5\ H_2$ (ethylidyne, Fig. 4(b))	−99	−117	−115
$Pt_{10} + C_2H_4 = Pt_{10}\text{-}CHCH_2 + 0.5H_2$ (vinyl, Fig. 7(b))	−53	−78	−73
$Pt_{10} + C_2H_4 = Pt_{10}\text{-}CHCH_2 + 0.5\ H_2$ (vinyl, Fig. 7(a))	−24	−49	−44
$Pt_{10} + C_2H_2 = Pt_{10}\text{-}C_2H_2$ (di-σ/π acetylene, Fig. 5(a))	−209	−209	−209
$Pt_{10} + C_2H_2 = Pt_{10}\text{-}C_2H_2$ (π acetylene, Fig. 5(c))	−88	−88	−88
$Pt_{10} + C_2H_2 = Pt_{10}\text{-}CCH_2$ (di-σ/π vinylidene, Fig. 5(b))	−274	−278	−280
$Pt_{10} + CH_4 = Pt_{10}\text{-}CH + 1.5\ H_2$ (Fig. 6(a))	102	54	64
$Pt_{10} + CH_4 = Pt_{10}\text{-}CH_2 + H_2$ (Fig. 6(b))	118	81	88
$Pt_{10} + CH_4 = Pt_{10}\text{-}CH_3 + 0.5\ H_2$ (methyl, Fig. 6(c))	6	−15	−10
$Pt_{10} + C_2H_6 = Pt_{10}\text{-}C_2H_5 + 0.5\ H_2$ (ethyl, Fig. 6(d))	1	−20	−15
$Pt_{10} + C_2H_4 = Pt_{10}\text{-}CHCH_3$ (ethylidene, Fig. 8)	−87	−95	−94

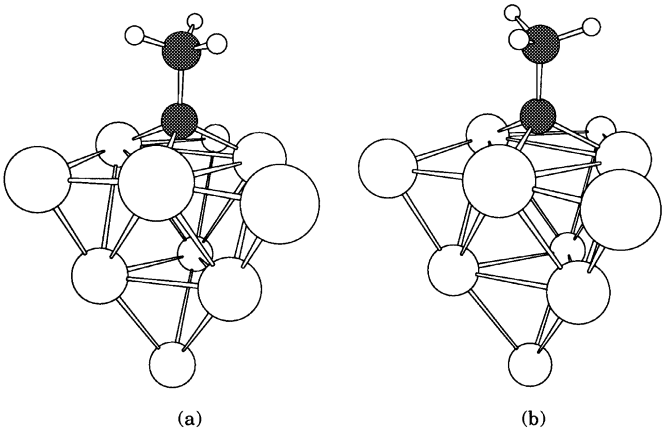

FIG. 4. Structural models for two modes of ethylidyne species on Pt_{10} clusters for which the hydrogen atoms point toward (a) bridge and (b) atop positions.

integral heat of adsorption. Since surface diffusion allows equilibrated adsorption of ethylene on a single crystal surface, the observed heat of King and co-workers is more representative for the formation of ethylidyne species on Pt (39).

Acetylene-Pt_{10}. Acetylene adsorption on various surfaces has been studied by different theoretical techniques, including extended Huckel theory (72, 73). Molecularly adsorbed acetylene prefers a high coordination triangular site (27), and the molecular geometry resulting from our DFT calculations is shown in Fig. 5a. The calculated C-C bond length is 1.41 Å, indicating rehybridization from sp towards sp^3 hybridization. This calculated bond length is in agreement with the experimental value of 1.35 Å, based on vibrational data and the values of 1.35–1.39 Å based on UPS measurements (30). The C-C-H angle is 121°, in agreement with the experimental values of 120–132° based on UPS level positions (30). The calculated heat of acetylene adsorption is −209 kJ/mol to form the molecularly adsorbed species shown in Fig. 5a. The measured heat of acetylene adsorption on Pt powder at 173 K is equal to −210 kJ/mol (35), as shown in Table 2. At temperatures lower than 250 K, acetylene has been shown to adsorb molecularly with its C-C axis oriented parallel to the platinum surface (23). On a Pt(111) surface, acetylene adsorbs preferentially in threefold hollow sites and forms two σ-bonds and one π-bond to three platinum atoms. Therefore, the measured heat of −210 kJ/mol is most likely related to formation of the di-σ/π-acetylene (μ_3, η^2-ethyne) species on a threefold platinum site.

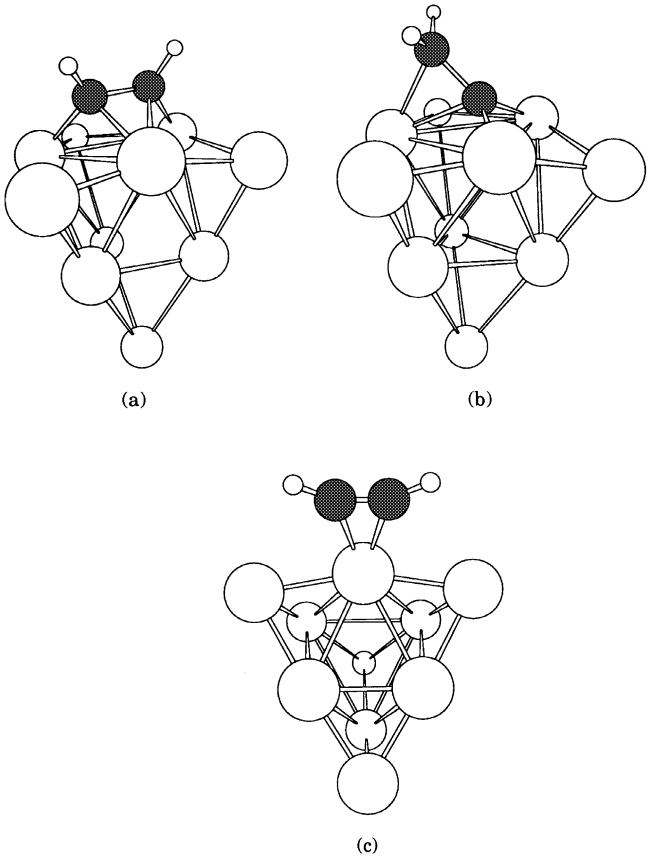

FIG. 5. Structural models for species formed from acetylene adsorption on Pt_{10} clusters: (a) di-σ/π-adsorbed acetylene, (b) di-σ/π vinylidene species, and (c) π-adsorbed acetylene.

At temperatures higher than ∼280 K, acetylene has been shown to adsorb with its C-C axis tilted away from the platinum surface. Different species such as vinylidene, ethylidyne, and di-σ/π-vinylidene have been proposed to form. Figure 5b shows the optimized geometry of a CCH_2 species on Pt_{10}, oriented with its C-C axis aligned at an angle to the surface. This species represents a di-σ/π-vinylidene species (μ_3, η^2-vinylidene) with both hydrogen atoms on a single carbon atom. The Pt-C bond lengths involved in σ-bonding are 1.92 Å, while the Pt-C bond length involved in π-bonding is 2.00 Å. The C-C bond length is calculated to be 1.44 Å, indicating rehybridization towards sp^3 hybridization. NMR studies of acetylene adsorption on small platinum particles at room temperature have shown existence of CCH_2 (77%) and HCCH (23%) species; and, the C-C bond length of the CCH_2 species was determined to be 1.44 Å (32), in agreement with our calculated value. The calculated heat of acetylene adsorption to form this species is −278 kJ/mol at 298 K (see Table 3).

We have attempted to calculate the energetics of μ_2-vinylidene species on Pt, for which the C-C double bond is retained (i.e., corresponding to a C-C bond length of 1.34 Å). A constrained optimization was thus carried out with the C-C bond length fixed at 1.34 Å. This procedure resulted in a species similar to that in Fig. 5b, and the heat of adsorption for this species from acetylene was calculated to be −262 kJ/mol. Hence, we find that the CCH_2 species in Fig. 5b is the most stable among the acetylene isomers.

Figure 5c shows a π-bonded form of acetylene (η^2-ethyne) adsorbed on an atop site of the Pt_{10} cluster. The C-C bond length is 1.25 Å and the heat of adsorption of this species is calculated to be −88 kJ/mol. Hence, our calculations predict the existence of a weakly adsorbed, π-bonded acetylene species, even though to the best of our knowledge there is no experimental evidence for such a species.

King and co-workers have reported an initial heat of −205 kJ/mol for ethylene adsorption on Pt(110)(2×1) at room temperature (39). These investigators attributed this heat to the formation of a di-σ/π vinylidene species on the platinum surface. This reported heat from ethylene adsorption corresponds to a heat of −290 kJ/mol for the adsorption of acetylene (assuming that the heat of dehydrogenation of ethylene to acetylene is 175 kJ/mol (74) at 298 K and that the heat of dihydrogen adsorption on Pt is equal to −90 kJ/mol). Table 2 compares the experimental and calculated heats of

formation of di-σ/π vinylidene species from acetylene at room temperature.

Effects of cluster approach. It is recognized that there are limitations of the cluster approach employed in the theoretical calculations. The primary assumption behind this approach is that chemisorption is a local phenomenon which is primarily affected by the nearby structure. Accordingly, the predicted properties will be affected by the spin state, cluster size and shape, orientation of the adsorbate on the cluster, as well as the level of theory and chosen basis set.

We have used the singlet electronic configuration of the Pt_{10} cluster to calculate the heats of adsorption of various species reported in this paper. A recent DFT study (75) reported that the ground state for a similar Pt_{10} cluster was a nonet (i.e., multiplicity of 9). We also find that the nonet electronic state is more stable than the singlet by 116 kJ/mol. The most stable electronic configuration became a singlet, however, when an oxygen atom was adsorbed on the Pt_{10} cluster (75). Since most practical platinum catalysts are supported on oxide surfaces, it is probable that the singlet state may be more appropriate to use in DFT calculations to model reactions on supported Pt catalysts. We have also carried out DFT calculations on larger Pt clusters, containing 14 and 23 Pt atoms. The most stable electronic state is a pentet for the Pt_{14} cluster, and it is a singlet for the Pt_{23} cluster. The ground state for bulk platinum should be a singlet, since this metal is not magnetic.

The existing literature has guided our search for the adsorption sites and the orientation of the adsorbate on these sites. Adsorption sites were limited to the central six atoms of the Pt cluster (coordination number of 6). Adsorption on the four corner atoms in the cluster were not considered, since their coordination number is 3 and may have different electronic density.

The Pt-Pt bond distances were not constrained for the Pt_{10} cluster, since relaxation and adsorption-induced reconstruction effects are common for small particles (50–52). We have studied the adsorption of some key species on the unrelaxed Pt_{10} cluster with Pt-Pt bond lengths maintained at 2.77 Å. It was observed that the predicted heats of adsorption of ethylidyne, di-σ-adsorbed ethylene, and π-adsorbed ethylene were more exothermic on the unrelaxed cluster by 46, 6, and 24 kJ/mol, respectively.

We have investigated the effect of using a smaller basis set on the predicted energetics for our DFT calculations involving Pt_{10} clusters. In particular, we used the LAV3P basis set to study the formation of ethylidyne species and di-σ/π-adsorbed acetylene species. This smaller basis set uses a pseudo-potential to replace all core electrons of Pt atoms, including the outermost core electrons, leaving Pt with 10 electrons that are treated explicitly. The 6–31G** basis set is retained on all C and H atoms. The calculated heat of formation of ethylidyne species from ethylene adsorption with evolution of gaseous dihydrogen is −50 kJ/mol, and the heat of adsorption of acetylene to give the di-σ/π-adsorbed species is −155 kJ/mol. These values are significantly different from the values of −127 kJ/mol and −209 kJ/mol, respectively, obtained by including the outermost core electrons explicitly in the calculations.

Hydrocarbon fragments-Pt_{10}. In the previous sections we have compared the results from DFT calculations with experimental results for various well-defined surface species that are formed during the adsorption of ethylene and acetylene on platinum. Since we have found that DFT calculations using Pt_{10} clusters give reasonable geometries and energies for these surface species where extensive experimental data are available, we now use DFT calculations on Pt_{10} clusters to model hydrocarbon fragments on platinum for which detailed experimental data are not yet available. As noted earlier, this approach is employed to provide estimates for various reaction intermediates that may be involved in ethane hydrogenolysis on Pt.

Figure 6a–c shows optimized geometries for CH, CH_2, and CH_3 fragments on the Pt_{10} cluster, respectively. We find that CH, CH_2, and CH_3 species prefer the threefold hollow site, twofold bridge site, and onefold atop site, respectively. It appears that carbon binds at a site that preserves its

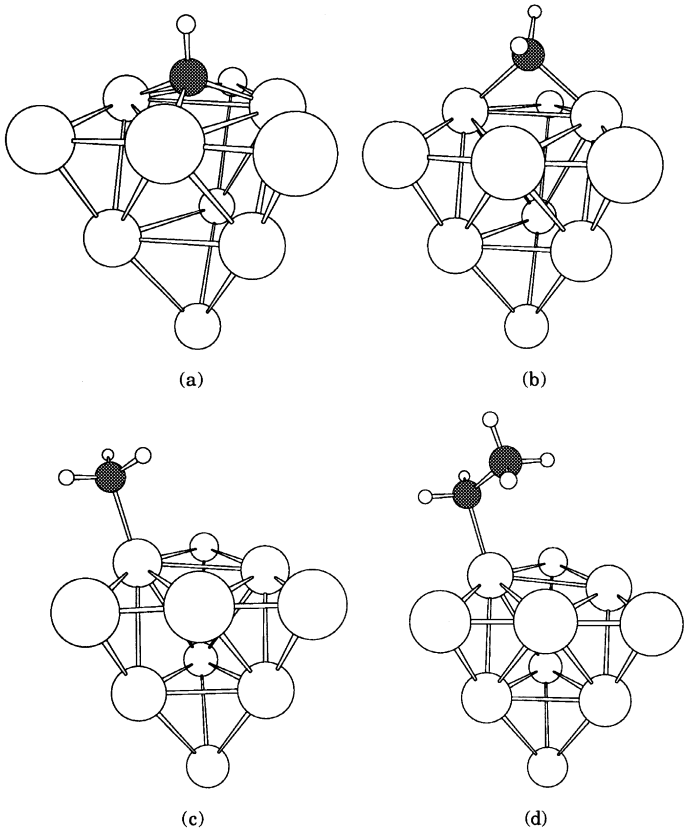

FIG. 6. Structural models for CH, CH_2, CH_3, and C_2H_5 species adsorbed on Pt_{10} clusters.

tetrahedral geometry and saturates its coordination. This observation is in agreement with previous theoretical studies using extended Huckel theory and discrete variational Xα theory (76). The Pt-C distances in adsorbed CH, CH_2, and CH_3 species are 1.95, 2.01, and 2.05 Å, respectively. The C-H bond lengths in all species are 1.09 Å, and the HCH angles are near 110°, indicating a tetrahedral structure for all species. The calculated heats of methane adsorption with evolution of gas phase dihydrogen are given in Table 3 . The energies of these CH_n species are in agreement with results from earlier theoretical studies (68, 77). The geometrical parameters, such as bond lengths, calculated in the present DFT study should be more accurate than those obtained in previously reported extended Huckel theory calculations, which are known to give inaccurate bond lengths.

Ethane may adsorb dissociatively on platinum to form adsorbed ethyl species and adsorbed hydrogen. The optimized geometry of an ethyl species on Pt_{10} is shown in Fig. 6d. This species adsorbs on an atop site, similar to a methyl group. The ethyl species is similar to gas phase ethane, i.e., the C-C and C-H bond lengths are 1.52 and 1.1 Å, respectively, and the HCC angle is 109°. The Pt-C distance is 2.06 Å, which is longer than the distances in CH_n species.

Other possible reactive intermediate are vinyl species, $CHCH_2$. Two configurations for these species are shown in Fig. 7. In the first isomer (Fig. 7a), the vinyl species is adsorbed on an atop site, as reported in an earlier theoretical study. This species is similar to gas phase ethylene, with a C-C bond length of 1.34 Å and a CCH angle of 120°. The Pt-C distance is 1.98 Å. The second isomer (Fig. 7b) for the vinyl species is more stable, and it is located on a threefold site. This vinyl species (μ_3, η^2-vinyl) has rehybridized to sp^3 hybridization, e.g., the C-C bond length is 1.50 Å. The Pt-C bond lengths for this species, associated with three platinum atoms, are 2.03–2.06 Å. The calculated heats of formation of these species from ethylene are shown in Table 3.

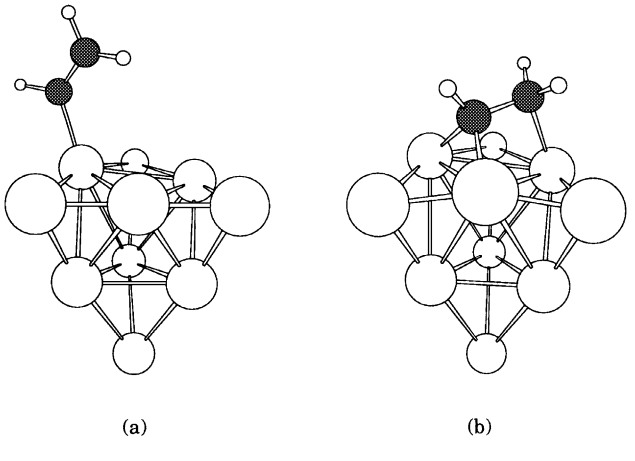

FIG. 7. Structural models for two modes of vinyl species adsorbed on Pt_{10} clusters: (a) vinyl, (b) μ_3, η^2-vinyl.

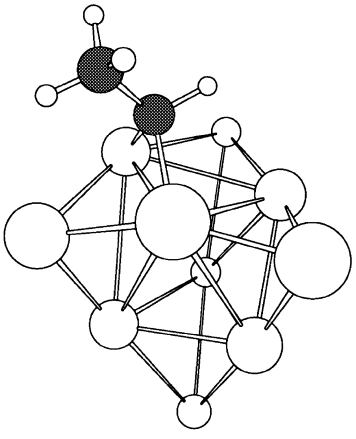

FIG. 8. Structural model for ethylidene species species adsorbed on a Pt_{10} cluster.

Another species that may form on Pt is the ethylidene species, $CHCH_3$ (μ_2-ethylidene). This species has been postulated to be an intermediate for the formation of ethylidyne species (CCH_3) on the Pt(111) surface. The optimized geometry for ethylidene species on the Pt_{10} cluster is shown in Fig. 8. The calculated heat of C_2H_4 adsorption to form ethylidene species is −87 kJ/mol. The calculated C-C bond length is 1.51 Å.

Application of Results for Ethane Hydrogenolysis

The results from the DFT calculations of the present study provide information about the energetics for various hydrocarbon fragments that may be involved in ethane hydrogenolysis on platinum. Importantly, this energetic information can be used to constrain the parameters that are used in kinetic models, based on elementary steps, to fit reaction kinetics data. In most kinetic models that have been used in this respect for ethane hydrogenolysis on Pt (11, 78), the adsorption of ethane is generally assumed to be quasi-equilibrated, leading to the formation of an adsorbed C_2H_x species which undergoes the rate-determining cleavage of the C-C bond. The quasi-equilibrated formation of this dehydrogenated C_2H_x species can be written as

$$C_2H_6 + * \rightleftharpoons C_2H_x* + (6-x)/2\ H_2.$$

Table 4 shows the heats of reactions to form different C_2H_x species on platinum using the energetics of Table 3 and gas phase enthalpies of formation (74). This table also shows entropy changes calculated from standard gas phase entropies (at 623 K and 1 atm) (74) and assuming that the adsorbed hydrocarbon species have no translational degrees of freedom (immobile adsorption) but retain their vibrational and rotational degrees of freedom (local entropy). Table 4 shows that the formation of C_2H_x species becomes

TABLE 4

Enthalpy and Standard Entropy Changes for Formation of C_2H_x Adsorbed Species on Pt at 623 K

Reaction	ΔH kJ/mol	ΔS° J/mol/K	$\theta_{C_2H_x}/\theta_{C_2H_2}$
$C_2H_6 + * \rightleftharpoons C_2H_5*$ (ethyl) $+ 0.5\ H_2$	−20	−90	7.2×10^{-6}
$C_2H_6 + * \rightleftharpoons C_2H_4*$ (di-σ-ethylene) $+ H_2$	−24	−33	1.6×10^{-2}
$C_2H_6 + * \rightleftharpoons C_2H_3*$ (ethylidyne) $+ 1.5\ H_2$	18	+32	2.7×10^{-2}
$C_2H_6 + * \rightleftharpoons C_2H_2*$ (di-σ/π-vinylidene) $+ 2\ H_2$	44	+97	1

Note. Standard state for gaseous species is 298 K and 1 atm. Surface species are assumed to be immobile.

more endothermic and the standard entropy change becomes more positive as more hydrogen atoms are removed from ethane. Accordingly, the formation of more highly dehydrogenated C_2H_x species is favored with increasing temperature. This information is critical for estimating the surface coverages by different hydrocarbon species during the ethane hydrogenolysis over platinum, as shown elsewhere (13). For example, di-σ/π-adsorbed vinylidene species, CCH_2, are predicted to be the most abundant surface species on Pt at typical reaction conditions for ethane hydrogenolysis, e.g., a temperature of 623 K for ethane and hydrogen pressures of 0.02 and 0.2 atm, respectively. Table 4 shows the relative coverages of other C_2H_x species compared to the CCH_2 coverage.

CONCLUSIONS

It is recognized that there are limitations of the cluster approach employed in theoretical calculations. Accordingly, microcalorimetric and spectroscopic results were applied to calibrate the theoretical methods by comparing results for observable, stable surface intermediates. Such a calibration establishes the appropriate geometry (e.g., cluster shape and size) and method (e.g., level of theory and basis set) to adequately described the desired chemistry.

The results from DFT calculations using 10-atom platinum clusters give structural and energetic information that generally agree with experimental data for various C_2 species on platinum. These comparisons have been made for di-σ-adsorbed ethylene, π-adsorbed ethylene, ethylidyne species (CCH_3), di-σ/π-adsorbed vinylidene species (CCH_2), and di-σ/π-adsorbed acetylene species. In general, the calculated heats of adsorption are within 20 kJ/mol of experimental values measured microcalorimetrically, and the calculated structural parameters are within several percent of experimentally values. This general agreement between experimental and theoretical results shown in Table 2 suggests that the present theoretical methods applied to a 10-atom platinum reasonably predict the interactions of C_2 hydrocarbon with platinum. Accordingly, these DFT calculations on Pt_{10} clusters were extended to predict the heats of interaction of various intermediates on Pt, including CH, CH_2, CH_3, C_2H_5, $CHCH_3$, and $CHCH_2$ species. The energetics for the formation of these species may be used as initial estimates in developing kinetic models for hydrocarbon conversion reactions on Pt, such as ethane hydrogenolysis.

ACKNOWLEDGMENTS

We wish to acknowledge the financial support for this work from the National Science Foundation and the National Center for Clean Industrial and Treatment Technologies.

REFERENCES

1. Gates, B. C., "Catalytic Chemistry." Wiley, New York, 1992.
2. Satterfield, C. N., "Heterogeneous Catalysis in Industrial Practice." McGraw–Hill, New York, 1991.
3. Masel, R. I., "Principles of Adsorption and Reaction on Solid Surfaces." Wiley, New York, 1996.
4. Somorjai, G. A., "Introduction to Surface Chemistry and Catalysis." Wiley, New York, 1994.
5. van Santen, R. A., and Neurock, M., *Catal. Rev. Sci. Eng.* **37**(4), 557 (1995).
6. van Santen, R. A., and Niemantsverdriet, J. W., "Chemical Kinetics and Catalysis." Plenum, New York, 1995.
7. Neurock, M., *Appl. Catal. A: General* **160**, 169 (1997).
8. Sautet, P., and Paul, J., *Catal. Lett.* **9**, 245 (1991).
9. Sinfelt, J. H., *Adv. Catal.* **23**, 91 (1973).
10. Bond, G. C., and Cunningham, R. H., *J. Catal.* **166**, 172 (1997).
11. Cimino, A., Boudart, M., and Taylor, H. S., *J. Am. Chem. Soc.* **58**, 96 (1954).
12. Goddard, S. A., Amiridis, M. D., Rekoske, J. E., Cardona-Martinez, N., and Dumesic, J. A., *J. Catal.* **117**, 155 (1989).
13. Cortright, R. D., Watwe, R. M., Spiewak, B. E., and Dumesic, J. A., *Catal. Today*, submitted.
14. Carter, E. A., and Koel, B. E., *Surf. Sci.* **226**, 339 (1990).
15. Benson, S. W., "Thermochemical Kinetics." Wiley, New York, 1976.
16. Cassuto, A., Kiss, J., and White, J. M., *Surf. Sci.* **255**, 289 (1991).
17. Cremer, P., Stanners, C., Niemantsverdriet, J. W., Shen, Y. R., and Somorjai, G., *Surf. Sci.* **328**, 111 (1995).
18. Demuth, J. E., *Surf. Sci.* **80**, 367 (1979).
19. Ibach, H., and Lehwald, S., *J. Vac. Sci. Technol.* **15**(2), 407 (1979).
20. Salmerón, M., and Somorjai, G. A., *J. Phys. Chem.* **86**, 341 (1982).
21. Demuth, J. E., *Surf. Sci.* **84**, 315 (1979).
22. Kesmodel, L. L., Dubois, L. H., and Somorjai, G. A., *J. Chem. Phys.* **70**(5), 2180 (1979).
23. Sheppard, N., and de la Cruz, C., *Adv. Catal.* **41**, 1 (1996).
24. Sheppard, N., *Ann. Rev. Phys. Chem.* **39**, 589 (1988).
25. Koestner, R. J., Van Hove, M. A., and Somorjai, G. A., *J. Phys. Chem.* **87**, 203 (1983).
26. Mehandru, S. P., and Anderson, A. B., *Appl. Surf. Sci.* **19**, 116 (1984).
27. Kesmodel, L. L., Baetzold, R. C., and Somorjai, G. A., *Surf. Sci.* **66**, 299 (1977).
28. Albert, M. R., Sneddon, L. G., Eberhardt, W., Greuter, F., Gustafsson, T., and Plummer, E. W., *Surf. Sci.* **120**, 19 (1982).
29. Megiris, C. E., Berlowitz, P., Butt, J. B., and Kung, H. H., *Surf. Sci.* **159**, 184 (1985).
30. Felter, T. E., and Weinberg, W. H., *Surf. Sci.* **103**, 265 (1981).
31. Rashidi, M., and Puddephatt, R. J., *J. Am. Chem. Soc.* **108**, 7111 (1986).

32. Wang, P.-K., Slichter, C. P., and Sinfelt, J. H., *Phys. Rev. Lett.* **53**(1), 82 (1984).
33. Avery, N. R., *Langmuir* **4**, 445 (1988).
34. Klug, C. A., Slichter, C. P., and Sinfelt, J. H., *J. Phys. Chem.* **95**, 2119 (1991).
35. Spiewak, B. E., Cortright, R. D., and Dumesic, J. A., *J. Catal.* **176**, 405 (1998).
36. Natal-Santiago, N. A., Podkolzin, S. G., Cortright, R. D., and Dumesic, J. A., *Catal. Lett.* **45**, 155 (1997).
37. Cortright, R. D., and Dumesic, J. A., *J. Catal.* **148**, 771 (1994).
38. Cortright, R. D., and Dumesic, J. A., *J. Catal.* **157**, 576 (1995).
39. Stuck, A., Wartnaby, C. E., Yeo, Y. Y., and King, D. A., *Phys. Rev. Lett.* **74**(4), 578 (1995).
40. Yeo, Y. Y., Wartnaby, C. E., and King, D. A., *Science* **268**, 1731 (1995).
41. Yeo, Y. Y., Stuck, A., Wartnaby, C. E., and King, D. A., *Chem. Phys. Lett.* **259**, 28 (1996).
42. van Santen, R. A., *in* "NATO ASI Series E: Applied Sciences—Chemisorption and Reactivity on Supported Clusters and Thin Films," Vol. 331, p. 331 (R. M. Lambert and G. Pacchioni, Eds.), Kluwer Academic, Trapani, Sicily, 1996.
43. Siegbahn, P. E. M., *Adv. Chem. Phys.* **93**, 333 (1996).
44. Paul, J. F., and Sautet, P., *in* "11th International Congress on Catalysis," Vol. 101, p. 1253 (J. W. Hightower, W. N. Delgass, E. Iglesia, and A. T. Bell, Eds.), Elsevier Science, New York, 1996.
45. Fahmi, A., and van Santen, R. A., *J. Phys. Chem.* **100**, 5676 (1996).
46. Ringnalda, M. N., *et al.* "PS-GVB," Schrodinger, Portland, OR, 1996.
47. Becke, A. D., *J. Chem. Phys.* **98**, 5648 (1993).
48. Hay, P. J., and Wadt, W. R., *J. Chem. Phys.* **82**, 299 (1985).
49. Hehre, W. J., Radom, L., Schleyer, P. v. R., and Pople, J. A., "Ab initio Molecular Orbital Theory." Wiley, New York, 1987.
50. Gallezot, P., *Surf. Sci.* **106**, 459 (1981).
51. Gallezot, P., and Bergeret, G., *J. Catal.* **72**, 294 (1981).
52. Moraweck, B., Clugnet, G., and Renouprez, A. J., *Surf. Sci.* **81**, L631 (1979).
53. Boys, S. F., and Bernardi, F., *Mol. Phys.* **19**, 553 (1970).
54. Carroll, J. J., and Weisshaar, J. C., *J. Phys. Chem.* **99**, 14388 (1995).
55. Watwe, R. M., Spiewak, B. E., Cortright, R. D., and Dumesic, J. A., *Catal. Lett.* **51**, 139 (1998).
56. Boyanov, B. I., and Morrison, T. I., *J. Phys. Chem.* **100**, 16310 (1996).
57. Vaarkamp, M., Modica, F. S., Miller, J. T., and Koningsberger, D. C., *J. Catal.* **144**, 611 (1993).
58. Tzou, M. S., Teo, B. K., and Sachtler, W. M. H., *J. Catal.* **113**, 220 (1988).
59. Kang, D., and Anderson, A., *Surf. Sci.* **155**, 639 (1985).
60. Maurice, V., and Minot, C., *Langmuir* **5**, 734 (1989).
61. Stohr, J., Gland, J. L., and Horsley, J. A., *Chem. Phys. Lett.* **105**, 332 (1984).
62. Stohr, J., Sette, F., and Johnson, A. L., *Phys. Rev. Lett.* **53**, 1684 (1984).
63. Döll, R., Gerken, C. A., Van Hove, M. A., and Somorjai, G. A., *Surf. Sci.* **374**(1–3), 151 (1997).
64. Cassuto, A., Mane, M., and Jupille, J., *Surf. Sci.* **249**, 8 (1991).
65. Yagasaki, E., and Masel, R. I., *Surf. Sci.* **226**, 51 (1990).
66. Yagasaki, E., and Masel, R. I., *Surf. Sci.* **222**, 430 (1989).
67. Paul, J. F., and Sautet, P., *J. Phys. Chem.* **98**, 10906 (1994).
68. Ditlevsen, P., Van Hove, M., and Somorjai, G., *Surf. Sci.* **292**, 267 (1993).
69. Shen, J., Hill, J. M., Watwe, R. M., Spiewak, B. E., and Dumesic, J. A., in preparation.
70. Starke, U., Barbieri, A., Materer, N., Van Hove, M. A., and Somorjai, G. A., *Surf. Sci.* **286**, 1 (1993).
71. Spiewak, B. E., and Dumesic, J. A., *Thermochim. Acta* **290**, 43 (1997).
72. Gavezzotti, A., and Simonetta, M., *Surf. Sci.* **99**, 453 (1980).
73. Anderson, A., and Hubbard, A., *Surf. Sci.* **99**, 384 (1980).
74. Stull, D. R., E. F. Westrum, J., and Sinke, G. C., "The Chemical Thermodynamics of Organic Compounds." Wiley, New York, 1969.
75. Chen, M., Bates, S. P., van Santen, R. A., and Friend, C. M., *J. Phys. Chem. B* **101**, 10051 (1997).
76. Feng, K., and Lin, Z., *Appl. Surf. Sci.* **72**, 139 (1993).
77. Minot, C., Van Hove, M., and Somorjai, G., *Surf. Sci.* **127**, 441 (1982).
78. Shang, S. B., and Kenney, C. N., *J. Catal.* **134**, 134 (1992).